

# Substituent and solvent effects on photoexcited states of functionalized fullerene [60]

Chuping Luo,<sup>a</sup> Mamoru Fujitsuka,<sup>a</sup> Akira Watanabe,<sup>a</sup> Osamu Ito,<sup>a\*</sup> Liangbing Gan,<sup>b</sup> Yanyi Huang<sup>b</sup> and Chun-Hui Huang<sup>b</sup>

<sup>a</sup> Institute for Chemical Reaction Science, Tohoku University, Katahira, Aoba-ku, Sendai, 980-77, Japan

<sup>b</sup> State Key Laboratory of Rare Earth Materials Chemistry and Applications, Peking University, Beijing 100871, China

Steady-state absorption/fluorescence spectra and time-resolved absorption/fluorescence spectra were measured to investigate the photoexcited states properties of *N*-methylpyrrolidinofullerenes C<sub>60</sub>[(C<sub>3</sub>H<sub>6</sub>N)R] [R = H (**1**), *p*-C<sub>6</sub>H<sub>4</sub>CHO (**2**), *p*-C<sub>6</sub>H<sub>4</sub>NO<sub>2</sub> (**3**), *p*-C<sub>6</sub>H<sub>4</sub>OMe (**4**), *p*-C<sub>6</sub>H<sub>4</sub>NMe<sub>2</sub> (**5**)]. Functionalization causes bandshifts to longer wavelength for absorption and fluorescence spectra, accompanied by enhancements in the fluorescence quantum yields in nonpolar solvents. The triplet (T) states of these derivatives show very similar properties (quantum yields, molar absorption coefficients and O<sub>2</sub> quenching) to C<sub>60</sub> whereas T–T absorption bands shift to short wavelength and the lowest triplet energies decrease compared with those of C<sub>60</sub>. Derivative **5**, which has a strong electron-donating group, shows a prominent solvent polarity effect on the fluorescent quantum yield and lifetime, and triplet formation, suggesting that intramolecular charge transfer takes place.

## Introduction

The photochemical and photophysical properties of fullerenes, such as C<sub>60</sub> and C<sub>70</sub>, have been widely investigated in recent years.<sup>1–6</sup> These spherical molecules are weakly fluorescent, are efficient <sup>3</sup>O<sub>2</sub> sensitizers and are also excellent electron acceptors and potential electron accumulators. These properties exhibit their potential applications in material and biological science.<sup>7–12</sup> Fullerene chemistry has also been developed by the introduction of various organic groups into the fullerenes,<sup>13–17</sup> these groups enhance the possibilities for the application of fullerenes. As they are one of the important classes, many pyrrolidinofullerenes have been synthesized;<sup>15–17</sup> some of which show excellent nonlinearity<sup>18–20</sup> and an efficient photocurrent response.<sup>21</sup> Introduction of electron donors stimulates electron transfer between the organic groups and the C<sub>60</sub> in the excited states.<sup>22–25</sup> Studies of photoexcited states are very helpful for understanding the mechanism of photocurrent generation and electron transfer.

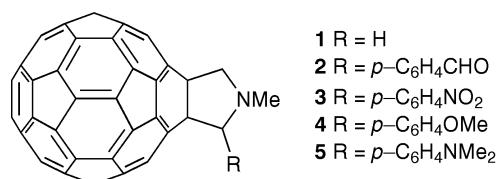
In the present paper, the photoexcited states of five *N*-methylpyrrolidinofullerenes (abbreviated as NMPF; Scheme 1) are systematically studied by using picosecond and nanosecond time-resolved spectroscopies. We expected that the excited states of these derivatives would be different from that of the pristine C<sub>60</sub>.

## Experimental

### Materials

C<sub>60</sub> (99.9%) was purchased from Texas Fullerenes. Benzophenone, β-carotene and iodoethane were of commercially available special grade. Solvents were of spectroscopic or HPLC grade.

The *N*-methylpyrrolidinofullerenes (NMPFs) were prepared according to the reaction shown in Scheme 2.<sup>13</sup> The products



Scheme 1

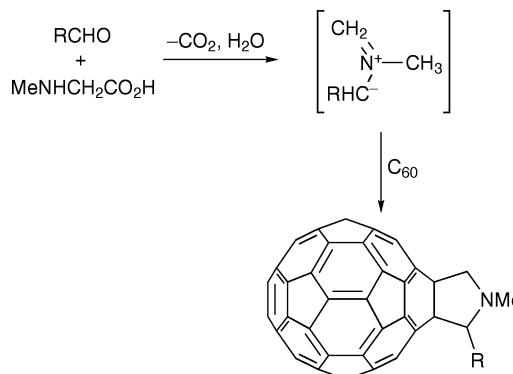
were characterized by field desorption mass spectrometry (FDMS), <sup>1</sup>H NMR (400 MHz) and <sup>13</sup>C NMR (100.6 MHz, Bruker, CS<sub>2</sub>); the details are given elsewhere.<sup>21,26</sup>

### Measurements

Transient-absorption and lifetime spectra were measured by using nanosecond laser-flash photolysis with second-harmonic (SHG) light (532 nm) from a Nd : YAG laser (6 ns FWHM) as the exciting source. For the transient absorption in the near-IR region, a Ge-avalanche photodiode module (Hamamatsu, C5331-SPL) attached to a monochromator was employed to detect the monitoring light from a pulsed Xe lamp (15 J pulse, 60 μs FWHM). For transient absorption in the visible region, which was used to determine the triplet–triplet (T–T) molar absorption coefficients, triplet quantum yields and oxygen quenching rates, a photomultiplier was used as the detector for monitoring the transmitted light from the continuous Xe lamp (150 W). The details of the experimental setup are described elsewhere.<sup>27</sup>

Fluorescence lifetimes were measured by a single-photon counting method using an argon ion laser pumped Ti : sapphire laser (Spectra-Physics, Tsunami) with a pulse selector, a harmonic generator and a streak scope (Hamamatsu, C4334-01).

Steady-state absorption spectra were recorded on a JASCO/V-570 spectrophotometer. Steady-state fluorescence



Scheme 2

spectra were measured on a Shimadzu RF-5300 PC spectrofluorophotometer with a photomultiplier effective in the visible and near-IR region. For determination of fluorescence quantum yields ( $\Phi_F$ ), an argon-deaerated toluene solution of  $C_{60}$  was used as a standard ( $\Phi_F = 3.2 \times 10^{-4}$ ).<sup>28</sup> Excitation wavelength was 420 nm after the absorbance of the samples and  $C_{60}$  was adjusted to 0.080 (in 1 cm quartz cell) at this wavelength. Phosphorescence spectra were measured in toluene with iodoethane (3 : 1) at 77 K.

## Results and Discussion

### Steady-state absorption spectra

Steady-state absorption spectra of  $C_{60}$  and NMPF in benzene at room temperature are shown in Fig. 1. The absorption spectra of the derivatives are different from their parent  $C_{60}$ . In the UV region, the derivatives show two bands at around 309 and 327 nm, whereas  $C_{60}$  shows two peaks at 334 and 337 nm. In the visible region, the derivatives exhibit different vibronic structures from  $C_{60}$ . Two distinct bands appear at 433 and *ca.* 705 nm for the derivatives that are thought to correspond to the electronic transition of  $C_{60}$  at 407 and 624 nm, respectively.<sup>29</sup> In addition, four weak broad bands can be distinguished over the ranges 450–500, 525–575, 600–625 and 630–655 nm for these derivatives. It is apparent that the groups introduced into the NMPFs have hyperchromic effects in the visible region, implying that the electronic forbidden transitions of  $C_{60}$  are loosened by the presence of the substituents owing to a reduction in the molecular symmetry. The representative absorption maxima are summarized in Table 1.

Although the absorption profiles are very similar for these derivatives, there are still slight differences. As shown in Table 1, the absorption bands at around 705 nm, which are caused

by a lowering of the icosahedral symmetry of  $C_{60}$ ,<sup>30</sup> show slight shifts among the derivatives. By taking derivative 1 as a reference, electron-withdrawing groups, such as CHO (in derivative 2) and  $NO_2$  (in derivative 3), have hypsochromic effects, *i.e.* from about 2 nm to short wavelength; whereas the electron-donating groups, such as OMe (in derivative 4) and  $NMe_2$  (in derivative 5), show bathochromic effects, *i.e.* from about 1 nm to long wavelength. Since the absorption bands at *ca.* 705 nm result from the functionalization of  $C_{60}$  by the extra organic groups, these small band shifts indicate that the transition of the  $C_{60}$  moiety is weakly influenced by the inductive effects of the introduced groups.

Solvents also have some effects on the electronic transitions of the NMPFs. As an example of this, the absorption spectra for derivative 5 in different solvents are shown in Fig. 2. In cyclohexane, the fine structures are relatively sharp, whereas the absorption bands in the range 600–700 nm are obscured in benzene and benzonitrile. In DMF solution, each band becomes more indistinct and new broad bands extend to 800–1000 nm, suggesting that interactions, such as charge transfer, between derivative 5 and the DMF molecules at ground state becomes significant. Similar phenomena were observed for the other derivatives and  $C_{60}$ .

### Steady-state fluorescence spectra

Fig. 3 shows the steady-state fluorescence spectra of  $C_{60}$  and its derivatives. In comparison with pristine  $C_{60}$ , the fluorescence intensities of the derivatives are several times higher, suggesting that breaking the symmetry of  $C_{60}$  results in an increase of emission intensity. The groups introduced also slightly affect the peak positions and emission intensities of the NMPFs. As shown in Table 1, the electron-withdrawing groups in derivatives 2 and 3 cause blue shift effects on the fluorescence maxima, while the electron-donating groups in

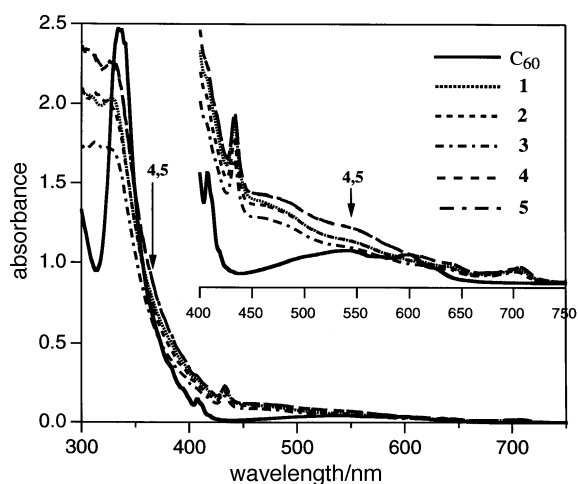


**Fig. 1** Absorption spectra of  $C_{60}$  and its derivatives 1–5 in benzene solution at room temperature (concentration,  $4.10 \times 10^{-5}$  mol dm<sup>-3</sup>; pathlength, 1 cm)

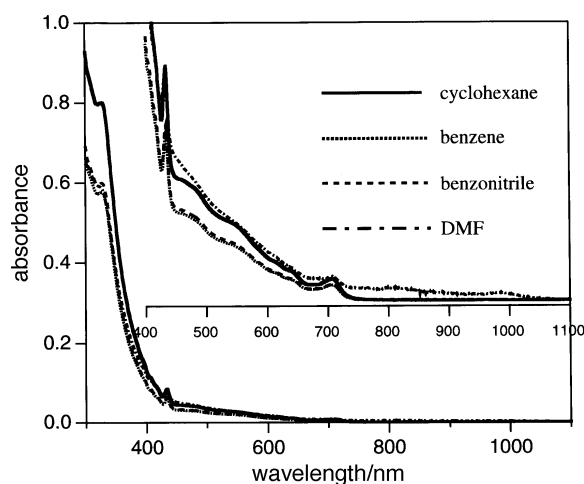


**Fig. 2** Absorption spectra for derivative 5 in different solvents at room temperature (concentration,  $1.56 \times 10^{-5}$  mol dm<sup>-3</sup>; pathlength, 1 cm)

**Table 1** Absorption and fluorescence parameters of  $C_{60}$  and its derivatives in benzene

	absorption band/nm	fluorescence band/nm	Stokes shift/cm <sup>-1</sup>	$E_s^*$ /eV
$C_{60}$	334, 337, 407, 540, 597, 624	697, 724	— <sup>b</sup>	1.99 <sup>c</sup>
1	309, 327, 433, 705	711, 788	120	1.74
2	312, 324, 433, 702	708, 787	120	1.75
3	313, 323, 433, 701	708, 785	141	1.75
4	311, 324, 433, 706	712, 788	120	1.74
5	309, 330, 433, 707	714, 792	139	1.74

<sup>a</sup>  $E_s^*$  denotes the excited singlet energy.

<sup>b</sup> The value should be a negligible one as reported in ref. 29. <sup>c</sup> Taken from ref. 1.

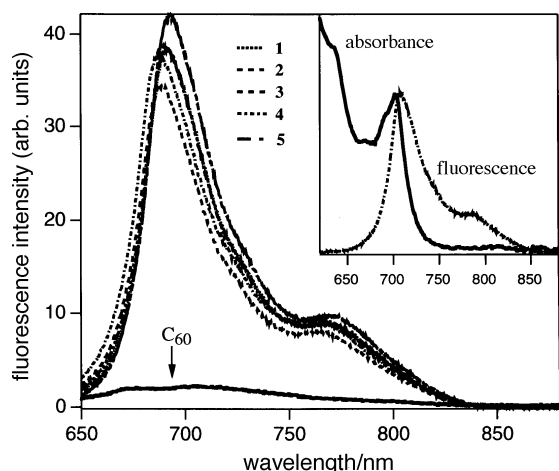


**Fig. 3** Fluorescence spectra of  $C_{60}$  and derivatives 1–5 in benzene solution ( $4.11 \times 10^{-5} \text{ mol dm}^{-3}$ ) at room temperature. The insert is a comparison of the absorption and fluorescence spectra of derivative 3 (excitation wavelength, 420 nm; pathlength, 1 cm).

derivatives 4 and 5 result in red-shift effects, as compared with derivative 1. However, the shifts are small, giving similar singlet energies as shown in Table 1. A good mirror image of the fluorescence and absorption of the NMPFs can be observed (as shown in Fig. 3). The Stokes shift depends on the groups introduced as well. For 3 and 5, the Stokes shifts are larger than for the others, suggesting that both strong electron-withdrawing and electron-donating groups affect the electronic potential energy curves in the excited and ground states.

Polar solvents cause intensive effects on the emission of derivative 5 with  $NMe_2$ , whereas for the other NMPFs the effects of the solvents are very small (Fig. 4). For derivative 3, the better resolved fluorescence peak at 700 nm in cyclohexane shifts to 708, 712 and 713 nm in benzene, benzonitrile and DMF, respectively, with a decreasing intensity, which might result from the stronger interaction between derivative 3 and the solvents. In cyclohexane, the Stokes shift of derivative 3 decreases to  $37 \text{ cm}^{-1}$ , indicating that the potential energy curve is solvent dependent as well.

#### Fluorescence quantum yields

Fluorescence quantum yields ( $\Phi_F$ ) for the NMPFs at room temperature were determined in reference to the reported one of  $C_{60}$  in toluene ( $3.2 \times 10^{-4}$ ).<sup>28</sup> As summarized in Table 2, the  $\Phi_F$  values range from  $1.05 \times 10^{-3}$  to  $1.18 \times 10^{-3}$  in benzene, and from  $0.5 \times 10^{-4}$  to  $8.1 \times 10^{-4}$  in benzonitrile. The  $\Phi_F$  values are very similar for each of the derivatives in either solvent except for derivative 5 in polar solvent.<sup>31</sup> In comparison with pristine  $C_{60}$ , all the  $\Phi_F$  values for the derivatives in benzene increase, because of the reduction of the structural symmetry of  $C_{60}$ .

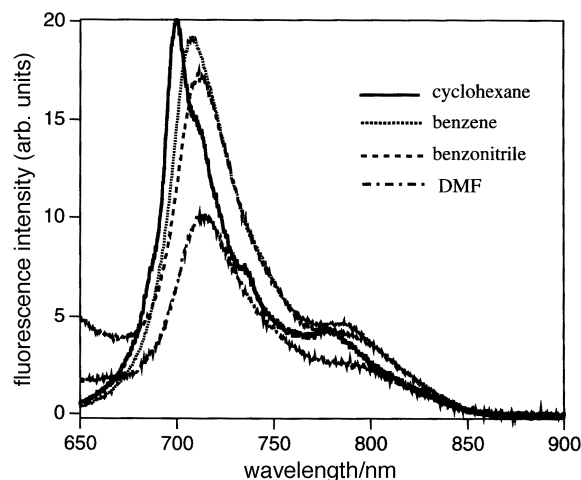


**Fig. 4** Fluorescence spectra for derivative 3 in different solvents ( $1.90 \times 10^{-5} \text{ mol dm}^{-3}$ ) at room temperature (excitation wavelength, 420 nm; pathlength, 1 cm)

#### Fluorescence lifetime

The time dependences of the fluorescence intensities of derivatives 1–4 (Fig. 5 and Table 2) are mono-exponential, giving fluorescence lifetimes ( $\tau_F$ ) of 1.1–1.3 ns in benzene and benzonitrile, which are very similar to that of  $C_{60}$ .<sup>32,33,34</sup> Therefore, the photoexcited singlet state of derivative 1–4 in polar solvents, such as benzonitrile, deactivates in the same way as in nonpolar solvent. However, a prominent decrease of  $\tau_F$  for derivative 5 in benzonitrile was observed (as shown in Table 2). The reason will be discussed in detail in a later section.

#### Transient absorption spectra

The transient absorption spectra of the NMPFs, measured using the nanosecond laser photolysis apparatus, are attributed to the triplet–triplet (T–T) absorption band (Table 2). The absorption maxima of the T–T transition of the NMPFs

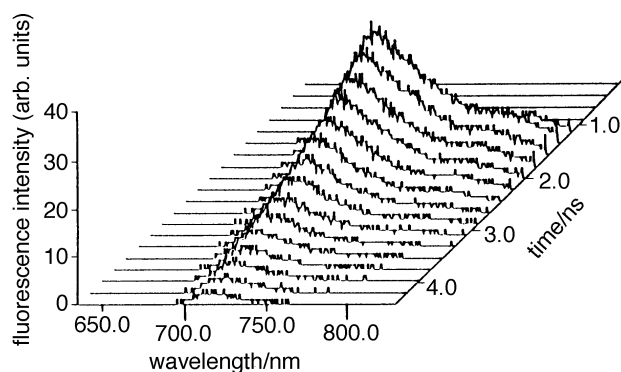


**Fig. 5** Time-resolved fluorescence of derivative 5 excited at 420 nm in argon bubbled benzene solution at room temperature

**Table 2** Parameters of singlet and triplet states of  $C_{60}$  and derivatives 1–5 in benzene and benzonitrile

solvent	$C_{60}$	1	2	3	4	5
$C_6H_6$						
$\Phi_F \times 10^4$	3.2 <sup>a</sup>	10.6	11.8	11.0	10.5	10.0
$\tau_F/\text{ns}$	1.245 <sup>b</sup>	1.3	1.2	1.3	1.3	1.2
$\lambda_T^{\text{max}}/\text{nm}$	750	690	700	680	680	680
$\tau_T/\mu\text{s}$	37	24	29	26	27	29
$C_6H_5CN$						
$\Phi_F \times 10^4$		6.0	4.8	6.7	8.1	0.5
$\tau_F/\text{ns}$		1.1	1.1	1.1	1.1	0.058
$\lambda_T^{\text{max}}/\text{nm}$	745	680	680	680	675	680
$\tau_T/\mu\text{s}$	26	27	30	30	29	11

<sup>a</sup> In toluene from ref. 28. <sup>b</sup> From ref. 3, 32, 33, 34.

are similar, but blue-shifted compared with that of C<sub>60</sub> itself (750 nm). The intensities of the T–T transition of 1–4 in benzonitrile are also very similar to those in benzene, whereas the intensity of 5 decreases significantly in benzonitrile (Fig. 6).

The triplet lifetimes ( $\tau_T$ ) of the derivatives in benzene are slightly shorter than that of C<sub>60</sub>. In benzonitrile, the  $\tau_T$  values for derivatives 1–4 are the same as those in benzene, whereas  $\tau_T$  for derivative 5 is much shorter than that in benzene.

Quantum yields ( $\Phi_T$ ) for triplet state formation *via* intersystem-crossing of C<sub>60</sub> and the NMPFs were determined in benzene by energy transfer to  $\beta$ -carotene using a 355 nm laser light as the excitation source. For these experiments, the concentrations of the derivatives are optically matched with benzophenone (BP), which was employed as a standard ( $\Phi_T = 1$ ) at 355 nm. The transient absorbance ( $\Delta A$ ) of the  $\beta$ -carotene triplet formed by the energy transfer from BP or from the derivatives triplet states was monitored at 530–550 nm ( $\Delta A^{\text{Ful}}$ ) and 680–700 nm ( $\Delta A^{\text{BP}}$ ), here the superscripts BP and Ful refer to benzophenone and fullerene, respectively. The following equation was used:<sup>35</sup>

$$\Phi_T^{\text{Ful}} = \Phi_T^{\text{BP}} \frac{\Delta A^{\text{Ful}}}{\Delta A^{\text{BP}}} \frac{k_{\text{obs}}^{\text{Ful}}}{k_{\text{obs}}^{\text{BP}} - k_0^{\text{Ful}}} \frac{k_{\text{obs}}^{\text{BP}} - k_0^{\text{BP}}}{k_{\text{obs}}^{\text{BP}}} \quad (1)$$

where  $k_{\text{obs}}$  is the rate constant for triplet energy transfer from BP or Ful to  $\beta$ -carotene and  $k_0$  is the rate constant for the decay of the BP or Ful triplet states in the absence of  $\beta$ -carotene. As  $\Delta A$  is a sensitized triplet formation of  $\beta$ -carotene, corrections are necessary to account for the decay of the donor triplets that occurs in competition with the energy transfer to  $\beta$ -carotene. These were performed.

The  $\Phi_T$  values for the derivatives in benzene are slightly smaller than that for pristine C<sub>60</sub> (Table 3). The triplet energy transfer rate constants  $k_{\text{et}}^{\text{Caro}}$  from these derivatives to  $\beta$ -carotene range from  $1.5 \times 10^9$  to  $2.4 \times 10^9 \text{ mol}^{-1} \text{ dm}^3 \text{ s}^{-1}$ , which are similar values to that of C<sub>60</sub> ( $2.8 \times 10^9 \text{ mol}^{-1} \text{ dm}^3 \text{ s}^{-1}$ ) (Table 3).

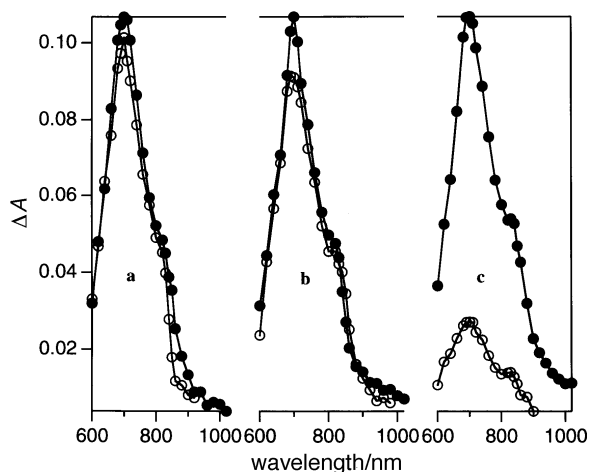


Fig. 6 Transient absorption spectra at 100 ns for derivative 2 (a, 2; b, 4; and c, 5) in argon bubbled benzene (●) and benzonitrile (○) at room temperature observed by nanosecond flash photolysis at 532 nm

The molar absorption coefficients ( $\epsilon_T$ ) of derivatives 1–5 were determined by comparison with that of  $\beta$ -carotene at 515 nm ( $\epsilon_T = 187000 \pm 5000 \text{ mol}^{-1} \text{ dm}^3 \text{ cm}^{-1}$ ).<sup>37,38</sup> Although in these actinometric experiments  $\beta$ -carotene absorbed a substantial amount of the 355 nm exciting light, such direct excitation did not result in any significant triplet formation of  $\beta$ -carotene, because of negligible triplet yield. As a consequence, the decrease of T–T absorbance of fullerenes ( $\Delta A_T^{\text{Ful}}$ ) equals the increase of T–T absorbance of  $\beta$ -carotene ( $\Delta A_T^{\text{Caro}}$ ), here Caro refers to  $\beta$ -carotene.

$$\Delta A_T^{\text{Ful}} / \Delta \epsilon_T^{\text{Ful}} = \Delta A_T^{\text{Caro}} / \Delta \epsilon_T^{\text{Caro}} \quad (2)$$

The molar absorption coefficients ( $\epsilon_T$ ) of the derivatives are similar to each other and are also close to that for C<sub>60</sub> (Table 3), thereby indicating that the triplet state properties of the derivatives are attributed by the fullerene moiety. The introduced groups slightly influence the  $\epsilon_T$  values.

The triplet states of the NMPFs can be strongly quenched by oxygen as can that for C<sub>60</sub> (Fig. 7).<sup>1</sup> The decay rates in aerated solution are 100 times faster than those in the solution bubbled by argon, and 10 times slower than those in oxygen-saturated solution. The quenching rates are slightly faster than that of C<sub>60</sub> except for derivative 3 (Table 3).

### Phosphorescence spectra

Although the excited singlet energies of the NMPFs are efficiently transferred to their triplet state by intersystem-crossing, the measurements of the phosphorescence spectra were still very difficult, implying that the radiative transitions between the different multiplicity states are principally forbidden. With an external heavy-atom effect in a mixed solvent of toluene and iodoethane (3 : 1 v/v), the fluorescence bands of these derivatives disappear, instead a new weak band appears at around 825 nm, which is attributed to a phosphorescence band (Fig. 8).

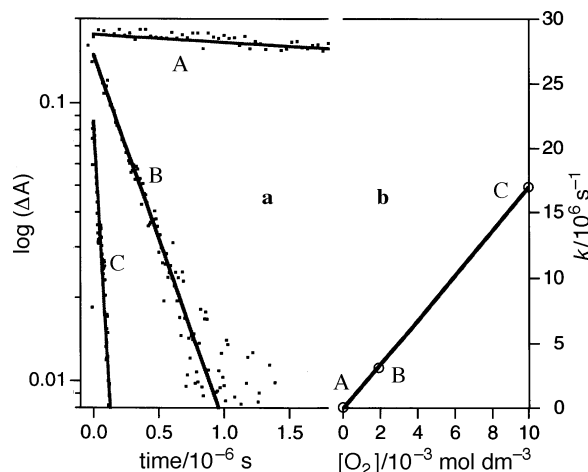


Fig. 7 a, Transient absorption decays of derivative 2 in benzene bubbled by: A, argon; B, air; and C, oxygen; b, relationship between triplet decay rate and oxygen concentration

Table 3 Triplet parameters of C<sub>60</sub> and its derivatives in benzene

	C <sub>60</sub>	1	2	3	4	5
$k_0/10^4 \text{ s}^{-1}$	3.0	4.1	3.5	3.7	3.7	3.6
$\Phi_T^{\text{Ful}}$	0.98	0.95	0.88	0.89	0.91	0.91
$k_{\text{et}}^{\text{Caro}}/10^9 \text{ mol}^{-1} \text{ dm}^3 \text{ s}^{-1}$	2.8	2.2	1.9	2.4	1.5	1.8
$\epsilon_T^{\text{Caro}}/\text{mol}^{-1} \text{ dm}^3 \text{ cm}^{-1}$	18 800	16 100	14 500	14 800	14 100	14 000
$k_q^{\text{O}_2}/10^9 \text{ mol}^{-1} \text{ dm}^3 \text{ s}^{-1}$	1.41	1.75	1.71	1.54	1.71	1.67
phosphorescence band/nm	788 <sup>b</sup>	826	824	824	826	826

<sup>a</sup>  $\pm 4200 \text{ mol}^{-1} \text{ dm}^3 \text{ cm}^{-1}$ . <sup>b</sup> Ref. 36.

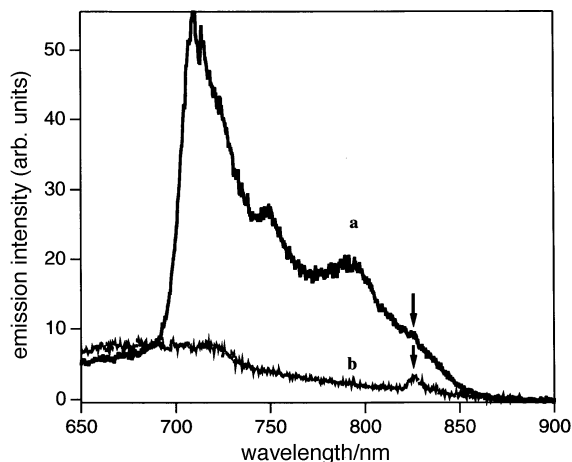


Fig. 8 Emission spectra for derivative 3 at 77 K [a, in toluene; and b, in toluene mixed with iodethane (3 : 1 v/v)]

The introduced groups also show a little effect on the positions of the phosphorescence bands. Derivatives 2 and 3 with electron-withdrawing groups, display a blue-shift of around 2 nm (Table 3). Consequently the triplet energy ( $E_T^*$ ) of these derivatives can be defined as 1.50 eV, which coincides with the reported values by others.<sup>39</sup> The lowest triplet energy level is only 0.25 eV lower than the lowest singlet energy level, which is smaller than that of  $C_{60}$  (0.42 eV).

#### Excited states deactivation of derivative 5 in polar solvents

In nonpolar solvents, such as cyclohexane and benzene, the excited state parameters of derivative 5 are very similar to those of other derivatives (Table 2). Therefore, derivative 5 undergoes the same deactivation pathways for the excited states as other derivatives (1–4). However, the situation changes significantly in high polar solvents.

In comparison with when in nonpolar solvents, the fluorescence intensities and quantum yield ( $\Phi_F$ ) of derivative 5 decrease markedly with an increase in solvent permittivity ( $\epsilon_r$ ) (as shown in Fig. 9a and Table 4), suggesting that an extra deactivation pathway competes with the radiative path.<sup>40</sup> Indeed, the fluorescence emissions in benzonitrile and DMF also show a rapid decay with a relative short lifetime (less than 90 ps) as shown in Fig. 9b. However, triplet state formation decreases significantly in polar solvent (Fig. 10), implying that the faster decay of the singlet state is not caused by efficient intersystem-crossing but by another deactivation pathway. The triplet lifetime ( $\tau_T$ ) of 5 in benzonitrile decreases by a factor of 1/2.5 compared with that in benzene (Table 4).

Table 4 Excited states parameters of derivative 5 in different solvents

solvent	$\epsilon_r^a$	$\Phi_F (\times 10^{-4})$	$\tau_F/\text{ns}$	$\tau_T/\mu\text{s}$
cyclohexane	2.023	11.1	1.2	31
benzene	2.275	10.0	1.2	29
Bz/Bn = 5 : 1 <sup>b</sup>	6.18	2.0	0.067	25
Bz/Bn = 1 : 1	13.99	1.4	0.056	13
Bz/Bn = 1 : 2	17.89	1.3	0.056	12
benzonitrile	25.70	0.5	0.058	11
Bz/DMF = 7 : 1	6.58	0.9	0.063	11
Bz/DMF = 4 : 1	9.16	0.7	0.083	7
Bz/DMF = 1 : 1	19.49	0.3	0.042	4
Bz/DMF = 1 : 4	29.82	0.2	0.050	<sup>c</sup>
DMF	36.71	0.2	0.040	<sup>c</sup>

<sup>a</sup>  $\epsilon_r$ : relative permittivity. <sup>b</sup> Bz: benzene; Bn: benzonitrile. <sup>c</sup> The instrumental response is too low to be analysed.

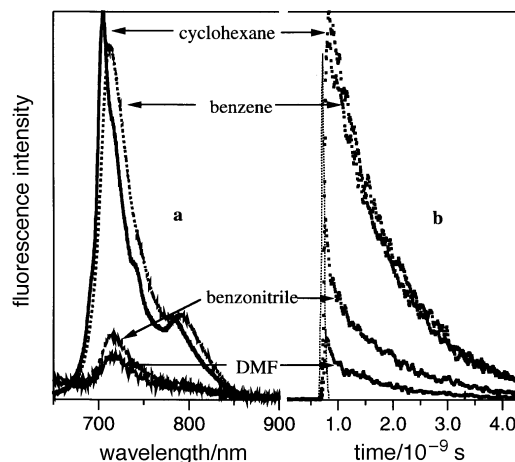


Fig. 9 Fluorescence spectra and decay profiles for derivative 5 in different solvents at room temperature: a, steady-state fluorescence; and b, time-resolved fluorescence decay. Laser pulse is also shown.

In comparison with the other derivatives, the only difference for derivative 5 is that it contains a stronger electron-donating group ( $NMe_2$ ). As the  $C_{60}$  moiety is a strong electron acceptor in the excited state,<sup>5,41</sup> the extra deactivating pathway is assigned to an intramolecular electron transfer from  $NMe_2$  to the excited singlet state of the  $C_{60}$  moiety, although the ion radicals cannot be found in our nanosecond transient absorption measurements.<sup>40</sup>

The fluorescence decay of derivative 5 in benzonitrile or DMF is not one component (Fig. 9b); the initial half of the intensity decay is very fast and the remaining half is slow, similar to that in a nonpolar solvent. The initial fast decay is attributed to the intramolecular electron transfer process. The later, relatively slow decay, might be due to the conformational change between the  $NMe_2$  moiety and the  $C_{60}$  moiety that accompanies the solvent redistribution.

Table 4 and Figure 11 show the influence of the relative permittivity ( $\epsilon_r$ ) of the solvent on  $\Phi_F$ ,  $\tau_F$  and  $\tau_T$ . For  $\Phi_F$ , a rapid drop was observed when benzonitrile and DMF were added to the nonpolar solvent benzene. DMF has a stronger effect on the drop of  $\Phi_F$  than benzonitrile. This can be attributed to the specific interaction between DMF and the fullerene molecules, as presumed from the steady-state absorption spectra in near-IR region (Fig. 2). For  $\tau_F$ , an effect similar to that for  $\Phi_F$  was observed. The polar solvent effects on the excited singlet state of 5 indicates that the intramolecular electron transfer process takes place in polar solvent with  $\epsilon_r > 7$ .

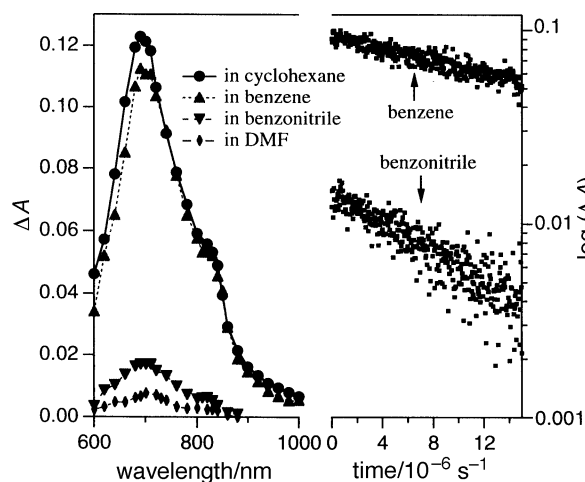
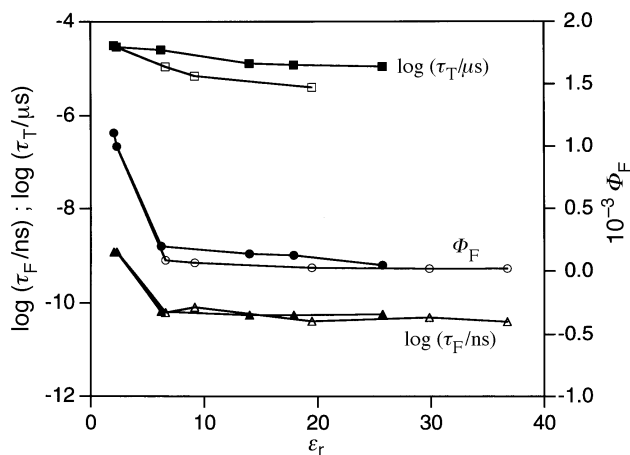


Fig. 10 Transient absorption spectra and decay profiles for derivative 5 in different solvents ( $5.7 \times 10^{-5} \text{ mol dm}^{-3}$ ) at room temperature observed by nanosecond flash photolysis at 532 nm



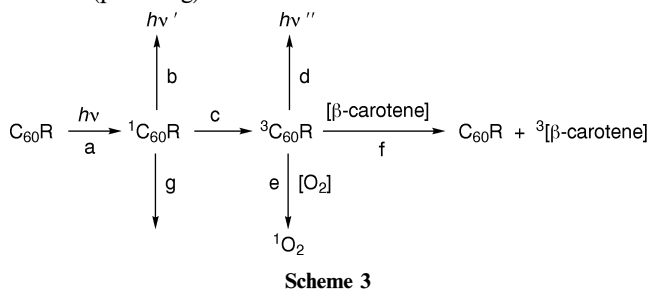
**Fig. 11** Relationship of relative permittivity ( $\epsilon_r$ ) vs.  $\Phi_F$  (●; ○),  $\log(\tau_F)$  (▲; △) and  $\log(\tau_T)$  (■; □) for derivative **5** in polar and non-polar solvents (filled symbols, in mixed solvents of benzene and benzonitrile; and open symbols, in mixed solvents of benzene and DMF)

Although the solvent polarity tends to decrease the  $\tau_T$  value, the size of the decrease was smaller than that for  $\tau_F$ . One of the reasons for the decrease in  $\tau_T$  might be an increase in the destruction of the forbidden process from  $T_1$  to  $S_0$ , by interaction with the solvents (including polar functions such as CN and amide groups).

## Conclusions

In comparison with  $C_{60}$ , a hyperchromic effect can be seen in the absorption spectra and an increase in fluorescence emission can be observed for the NMPFs, indicating that the symmetry reduction in the fullerene enhances the forbidden transition probability within the singlet states. The slight differences between the photoexcited states of derivatives **1–4** suggest that the electronic state of the  $C_{60}$  moiety is affected by the functional groups, with an inductive effect. However, derivative **5**, polar solvents strongly affect the electronic properties of the excited singlet.

The overall photoexcitation and deactivation pathways for the NMPFs can be seen as Scheme 3. After excitation to the lowest excited state (process a), the molecules deactivate *via* emission ( $h\nu'$ , process b) and *via* intersystem-crossing to the triplet state (process c); the triplet state is strongly quenched if either oxygen or other quenchers such as  $\beta$ -carotene exists. In high polar solvents, derivative **5** has an extra deactivation pathway from the singlet state *via* intramolecular electron transfer (process g).



The present work was partly supported by the Grant-in-Aid on Priority-Area-Research on 'Carbon Alloys' (No. 09243201) from the Ministry of Education, Science, Sports and Culture. This work was also supported in part by a grant from the Takeda Science Foundation.

## References

1 J. W. Arbogast, A. P. Darmanyan, C. S. Foote, Y. Rubin, F. N. Diederich, M. M. Alvarez, S. J. Anz and R. L. Whetten, *J. Phys. Chem.*, 1991, **95**, 11.

2 J. W. Arbogast and C. S. Foote, *J. Am. Chem. Soc.*, 1991, **113**, 8886.  
 3 T. W. Ebbesen, K. Tanigaki and S. Kuroshima, *Chem. Phys. Lett.*, 1991, **181**, 501.  
 4 D. M. Guldi, H. Hungerbuhler, E. Janata and K.-D. Asmus, *J. Phys. Chem.*, 1993, **97**, 11258.  
 5 C. S. Foote, in *Physics and Chemistry of the Fullerenes*, ed. K. Prassides, Kluwer Academic, Dordrecht, 1994, p.79.  
 6 O. Ito, *Res. Chem. Intermed.*, 1996, **23**, 389.  
 7 L. W. Tutt and A. Kost, *Nature (London)*, 1992, **356**, 225.  
 8 S. Shi, K. C. Khemani, Q. Li and F. Wudl, *J. Am. Chem. Soc.*, 1992, **114**, 10656.  
 9 A. Vasella, P. Uhlmann, C. A. A. Waldraff, F. Diederich and C. Thilgen, *Angew. Chem., Int. Ed. Engl.*, 1992, **31**, 1388.  
 10 K. E. Geckeler and A. Hirsch, *J. Am. Chem. Soc.*, 1993, **115**, 3850.  
 11 S. H. Friedman, D. L. DeCamp, R. P. Sijbesma, G. Srdanov, F. Wudl and G. L. Kenyon, *J. Am. Chem. Soc.*, 1993, **115**, 6506.  
 12 R. Sijbesma, G. Srdanov, F. Wudl, J. A. Castoro, C. Wilkins, S. H. Friedman, D. L. DeCamp and G. L. Kenyon, *J. Am. Chem. Soc.*, 1993, **115**, 6510.  
 13 A. Hirsch, *The Chemistry of Fullerenes*, Thieme, Stuttgart, 1994.  
 14 M. Maggini, G. Scorrano and M. Prato, *J. Am. Chem. Soc.*, 1993, **115**, 9798.  
 15 Q. Lu, D. I. Schuster and S. R. Wilson, *J. Org. Chem.*, 1996, **61**, 4764.  
 16 T. D. Ros and M. Prato, *J. Org. Chem.*, 1996, **61**, 9070.  
 17 F. Diederich and C. Thilgen, *Science*, 1996, **271**, 317.  
 18 M. Maggini, G. Scorrano, M. Prato, G. Brusatin, P. Innocenzi, M. Guglielmi, A. Renier, R. Signorini, M. Meneghetti and R. Bozio, *Adv. Mater.*, 1995, **7**, 404.  
 19 R. Signorini, M. Zerbetto, M. Meneghetti, R. Bozio, M. Maggini, C. De Faveri, M. Prato and G. Scorrano, *J. Chem. Soc., Chem. Commun.*, 1996, 1891.  
 20 Y.-P. Sun, E. J. Riggs and B. Liu, *Chem. Mater.*, 1997, **9**, 1268.  
 21 C. P. Luo, C. H. Huang, L. B. Gan, D. J. Zhou, W. S. Xia, Q. K. Zhuang, Y. Zhao and Y. Y. Huang, *J. Phys. Chem.*, 1996, **100**, 16685.  
 22 R. M. Williams, M. Koeberg, J. M. Lawson, Y.-Z. An, Y. Rubin, M. N. Paddonrow and J. W. Verhoeven, *J. Org. Chem.*, 1996, **61**, 5055.  
 23 D. M. Guldi, M. Maggini, G. Scorrano and M. Prato, *J. Am. Chem. Soc.*, 1997, **119**, 974.  
 24 H. Imahori, K. Hagiwara, M. Aoki, T. Akiyama, S. Taniguchi, T. Okada, M. Shirakara and Y. Sakata, *J. Am. Chem. Soc.*, 1996, **118**, 11771.  
 25 P. A. Liddell, D. Kuciauskas, J. P. Sumida, B. Nash, D. Nguyen, A. L. Moore, T. A. Moore and D. Gust, *J. Am. Chem. Soc.*, 1997, **119**, 1400.  
 26 D. J. Zhou, L. B. Gan, H. S. Tan, C. P. Luo, C. H. Huang, M. J. Lu, J. Q. Pan and Y. Wu, *Chin. Chem. Lett.*, 1995, **6**, 1033.  
 27 A. Watanabe and O. Ito, *J. Phys. Chem.*, 1994, **98**, 7736.  
 28 B. Ma and Y.-P. Sun, *J. Chem. Soc., Perkin Trans. 2*, 1996, 2157.  
 29 J. Catalán and J. Elguero, *J. Am. Chem. Soc.*, 1993, **115**, 9249.  
 30 L. Udvardi, P. R. Surján, J. Kürti and S. Pekker, *Synth. Met.*, 1995, **70**, 1377.  
 31 B. Ma, C. E. Bunker, R. Guduru, X.-F. Zhang and Y.-P. Sun, *J. Phys. Chem. A*, 1997, **101**, 5626.  
 32 D. Kim, M. Lee, Y. D. Suh and S. K. Kim, *J. Am. Chem. Soc.*, 1992, **114**, 4429.  
 33 D. K. Palit, A. V. Sapre, J. P. Mittal and C. N. R. Rao, *Chem. Phys. Lett.*, 1992, **195**, 1.  
 34 J. Song, F. Li, S. Qian, Y. Li, W. Peng, J. Zhou and Z. Yu, *Chin. Phys. Lett.*, 1994, **11**, 137.  
 35 C. V. Kumar, L. Qin and P. K. Das, *J. Chem. Soc., Faraday Trans. 2*, 1984, **80**, 783.  
 36 Y. Zeng, L. Biczok and H. Linschitz, *J. Phys. Chem.*, 1992, **96**, 5237.  
 37 D. S. Lawrence and D. G. Whitten, *Photochem. Photobiol.*, 1996, **64**, 923.  
 38 I. Carmichael and G. L. Hug, *J. Phys. Chem., Ref. Data* 1986, **15**, 1.  
 39 D. M. Guldi and K.-D. Asmus, *J. Phys. Chem. A*, 1997, **101**, 1472.  
 40 R. M. Williams, J. M. Zwier and J. W. Verhoeven, *J. Am. Chem. Soc.*, 1995, **117**, 4093.  
 41 J. W. Arbogast, C. S. Foote and M. Kao, *J. Am. Chem. Soc.*, 1992, **114**, 2277.

Paper 7/06672D; Received 15th September, 1997